Supplementary materials

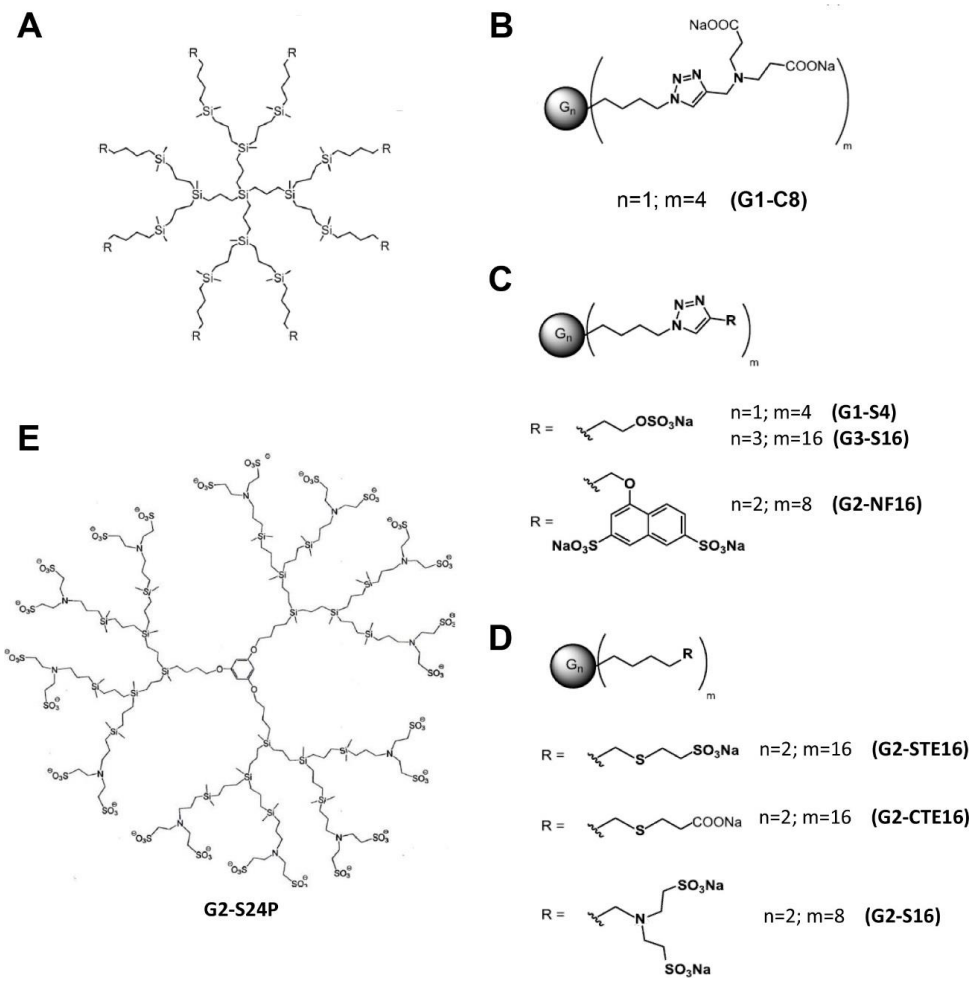

Figure S1 Structure of polyanionic carbosilane dendrimers.

Notes: (A) Representative scheme of a second-generation carbosilane dendrimer. **(B)** Structure of carboxylate-terminated dendrimers. First-generation carboxylate-functionalized G1-C8 ($C_{72}H_{124}N_{16}Na_8O_{16}Si_5$, MW: 1,794.20 g/mol). **(C)** Scheme of sulfated and naphthylsulfonated-decorated dendrimers. First-generation G1-S4 ($C_{52}H_{101}N_{12}Na_4O_{16}S_4Si_5$, MW: 1,509 g/mol); third-generation G3-S16 ($C_{256}H_{508}N_{48}Na_{16}O_{64}S_{16}Si_{29}$, MW: 6,978.41 g/mol) and second-generation G2-NF16 ($C_{184}H_{244}N_{24}Na_{16}O_{56}S_{16}Si_{13}$, MW: 4,934.02 g/mol). **(D)** Schematic structure of carbosilane dendrimers bearing sulfonate or carboxylate groups at their periphery synthesized by thiol-ene or Michael addition chemistry. Second-generation sulfonate-functionalized G2-S16

($C_{112}H_{244}N_8Na_{16}O_{48}S_{16}Si_{13}$, MW: 3,717.15 g/mol); second-generation via thiol-ene-synthesized G2-STE16 ($C_{144}H_{300}Na_{16}O_{48}S_{32}Si_{13}$, MW: 4,558.92 g/mol) and second-generation G2-CTE16 ($C_{128}H_{236}Na_{16}O_{32}S_{16}Si_{13}$, MW: 3,533.21 g/mol). **(E)** Polyphenolic core-sulfonated carbosilane dendrimer of second-generation G2-S24P ($C_{189}H_{402}N_{24}Na_{24}O_{75}S_{24}Si_{21}$, MW: 5,954.36 g/mol).

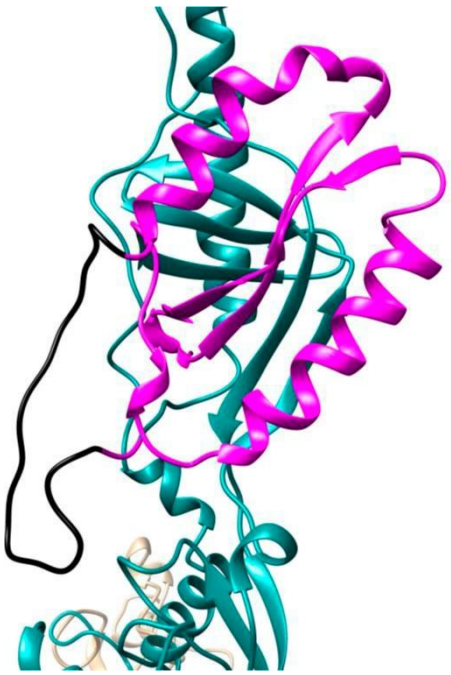

Figure S2 Detail of probable gB binding interface for the gH–gL.

Note: Part which is missing in "template" 4BOM structure and in gB HSV-2 strain 333 has primary sequence "PRNATPAPLREAPSANASV" is highlighted in black.

Score	Expect	Method	Identities	Positives	Gaps	Frame
1224 bits(3168)	0.0()	Compositional matrix adjust.	575/623(92%)	594/623(95%)	16/623(2%)	

Features:

```
Query  98    EIKVENADAQFYVCPPPTGATVVQFEQPRRCPTRPEGQNYTEGIAVVFKENIAPYKFKAT  157
            +IK EN DA FYVCPPPTGATVVQFEQPRRCPTRPEGQNYTEGIAVVFKENIAPYKFKAT
Sbjct  1     DIKAENTDANFYVCPPPTGATVVQFEQPRRCPTRPEGQNYTEGIAVVFKENIAPYKFKAT  60

Query  158   MYYKDVTVSQVWFGHRYSQFMGIFEDRAPVPFEEVIDKINAKGVCRSTAKYVRNNMETTA  217
            MYYKDVTVSQVWFGHRYSQFMGIFEDRAPVPFEEVIDKINAKGVCRSTAKYVRNN+ETTA
Sbjct  61    MYYKDVTVSQVWFGHRYSQFMGIFEDRAPVPFEEVIDKINAKGVCRSTAKYVRNNLETTA  120

Query  218   FHRDDHETDMELKPAKVATRTSRGWHTTDLKYNPSRVEAFHRYGTTVNCIVEEVDARSVY  277
            FHRDDHETDMELKPA  ATRTSRGWHTTDLKYNPSRVEAFHRYGTTVNCIVEEVDARSVY
Sbjct  121   FHRDDHETDMELKPANAATRTSRGWHTTDLKYNPSRVEAFHRYGTTVNCIVEEVDARSVY  180

Query  278   PYDEFVLATGDFVYMSPFYGYREGSHTEHTSYAADRFKQVDGFYARDLTTKARATSPTTR  337
            PYDEFVLATGDFVYMSPFYGYREGSHTEHTSYAADRFKQVDGFYARDLTTKARAT+PTTR
Sbjct  181   PYDEFVLATGDFVYMSPFYGYREGSHTEHTSYAADRFKQVDGFYARDLTTKARATAPTTR  240

Query  338   NLLTTPKFTVAWDWVPKRPAVCTMTKWQEVDEMLRAEYGGSFRFSSDAISTTFTTNLTQY  397
            NLLTTPKFTVAWDWVPKRP+VCTMTKWQEVDEMLR+EYGGSFRFSSDAISTTFTTNLT+Y
Sbjct  241   NLLTTPKFTVAWDWVPKRPSVCTMTKWQEVDEMLRSEYGGSFRFSSDAISTTFTTNLTEY  300

Query  398   SLSRVDLGDCIGRDAREAIDRMFARKYNATHIKVGQPQYYLATGGFLIAYQPLLSNTLAE  457
             LSRVDLGDCIG+DAR+A+DR+FAR+YNATHIKVGQPQYYLA GGFLIAYQPLLSNTLAE
Sbjct  301   PLSRVDLGDCIGKDARDAMDRIFARRYNATHIKVGQPQYYLANGGFLIAYQPLLSNTLAE  360

Query  458   LYVREYMREQDRKPRNATPAPLREAPSANASVERIKTTSSIEFARLQFTYNHIQRHVNDM  517
            LYVRE++REQ RKP                  VERIKTTSSIEFARLQFTYNHIQRHVNDM
Sbjct  361   LYVREHLREQSRKP----------------PVERIKTTSSIEFARLQFTYNHIQRHVNDM  404

Query  518   LGRIAVAWCELQNHELTLWNEARKLNPNAIASATVGRRVSARMLGDVMAVSTCVPVAPDN  577
            LGR+A+AWCELQNHELTLWNEARKLNPNAIAS TVGRRVSARMLGDVMAVSTCVPVA DN
Sbjct  405   LGRVAIAWCELQNHELTLWNEARKLNPNAIASVTVGRRVSARMLGDVMAVSTCVPVAADN  464

Query  578   VIVQNSMRVSSRPGTCYSRPLVSFRYEDQGPLIEGQLGENNELRLTRDALEPCTVGHRRY  637
            VIVQNSMR+SSRPG CYSRPLVSFRYEDQGPL+EGQLGENNELRLTRDA+EPCTVGHRRY
Sbjct  465   VIVQNSMRISSRPGACYSRPLVSFRYEDQGPLVEGQLGENNELRLTRDAIEPCTVGHRRY  524

Query  638   FIFGGGYVYFEEYAYSHQLSRADVTTVSTFIDLNITMLEDHEFVPLEVYTRHEIKDSGLL  697
            F FGGGYVYFEEYAYSHQLSRAD+TTVSTFIDLNITMLEDHEFVPLEVYTRHEIKDSGLL
Sbjct  525   FTFGGGYVYFEEYAYSHQLSRADITTVSTFIDLNITMLEDHEFVPLEVYTRHEIKDSGLL  584

Query  698   DYTEVQRRNQLHDLRFADIDTVI  720
            DYTEVQRRNQLHDLRFADIDTVI
Sbjct  585   DYTEVQRRNQLHDLRFADIDTVI  607
```

Figure S3 Comparison of the primary amino acid sequences of HSV-2, strain 333, amino acids 98–720 (Query) and gB from the experimental structure 4BOM (Sbjct). Middle record is composed of amino acids, which are identical in Query and Subject. Label “+” means that amino acids on that position in both sequences are different but that they are similar (eg, positively/negatively charged). Spaces (or “−“) means missing residue.

Score	Expect	Method	Identities	Positives	Gaps	Frame
1224 bits(3168)	0.0()	Compositional matrix adjust.	575/623(92%)	594/623(95%)	16/623(2%)	

Features:

```
Query  98    EIKVENADAQFYVCPPPTGATVVQFEQPRRCPTRPEGQNYTEGIAVVFKENIAPYKFKAT  157
            +IK EN DA FYVCPPPTGATVVQFEQPRRCPTRPEGQNYTEGIAVVFKENIAPYKFKAT
Sbjct  1     DIKAENTDANFYVCPPPTGATVVQFEQPRRCPTRPEGQNYTEGIAVVFKENIAPYKFKAT  60

Query  158   MYYKDVTVSQVWFGHRYSQFMGIFEDRAPVPFEEVIDKINAKGVCRSTAKYVRNNMETTA  217
            MYYKDVTVSQVWFGHRYSQFMGIFEDRAPVPFEEVIDKINAKGVCRSTAKYVRNN+ETTA
Sbjct  61    MYYKDVTVSQVWFGHRYSQFMGIFEDRAPVPFEEVIDKINAKGVCRSTAKYVRNNLETTA  120

Query  218   FHRDDHETDMELKPAKVATRTSRGWHTTDLKYNPSRVEAFHRYGTTVNCIVEEVDARSVY  277
            FHRDDHETDMELKPA  ATRTSRGWHTTDLKYNPSRVEAFHRYGTTVNCIVEEVDARSVY
Sbjct  121   FHRDDHETDMELKPANAATRTSRGWHTTDLKYNPSRVEAFHRYGTTVNCIVEEVDARSVY  180

Query  278   PYDEFVLATGDFVYMSPFYGYREGSHTEHTSYAADRFKQVDGFYARDLTTKARATSPTTR  337
            PYDEFVLATGDFVYMSPFYGYREGSHTEHTSYAADRFKQVDGFYARDLTTKARAT+PTTR
Sbjct  181   PYDEFVLATGDFVYMSPFYGYREGSHTEHTSYAADRFKQVDGFYARDLTTKARATAPTTR  240

Query  338   NLLTTPKFTVAWDWVPKRPAVCTMTKWQEVDEMLRAEYGGSFRFSSDAISTTFTTNLTQY  397
            NLLTTPKFTVAWDWVPKRP+VCTMTKWQEVDEMLR+EYGGSFRFSSDAISTTFTTNLT+Y
Sbjct  241   NLLTTPKFTVAWDWVPKRPSVCTMTKWQEVDEMLRSEYGGSFRFSSDAISTTFTTNLTEY  300

Query  398   SLSRVDLGDCIGRDAREAIDRMFARKYNATHIKVGQPQYYLATGGFLIAYQPLLSNTLAE  457
             LSRVDLGDCIG+DAR+A+DR+FAR+YNATHIKVGQPQYYLA GGFLIAYQPLLSNTLAE
Sbjct  301   PLSRVDLGDCIGKDARDAMDRIFARRYNATHIKVGQPQYYLANGGFLIAYQPLLSNTLAE  360

Query  458   LYVREYMREQDRKPRNATPAPLREAPSANASVERIKTTSSIEFARLQFTYNHIQRHVNDM  517
            LYVRE++REQ RKP                  VERIKTTSSIEFARLQFTYNHIQRHVNDM
Sbjct  361   LYVREHLREQSRKP----------------PVERIKTTSSIEFARLQFTYNHIQRHVNDM  404

Query  518   LGRIAVAWCELQNHELTLWNEARKLNPNAIASATVGRRVSARMLGDVMAVSTCVPVAPDN  577
            LGR+A+AWCELQNHELTLWNEARKLNPNAIAS TVGRRVSARMLGDVMAVSTCVPVA DN
Sbjct  405   LGRVAIAWCELQNHELTLWNEARKLNPNAIASVTVGRRVSARMLGDVMAVSTCVPVAADN  464

Query  578   VIVQNSMRVSSRPGTCYSRPLVSFRYEDQGPLIEGQLGENNELRLTRDALEPCTVGHRRY  637
            VIVQNSMR+SSRPG CYSRPLVSFRYEDQGPL+EGQLGENNELRLTRDA+EPCTVGHRRY
Sbjct  465   VIVQNSMRISSRPGACYSRPLVSFRYEDQGPLVEGQLGENNELRLTRDAIEPCTVGHRRY  524

Query  638   FIFGGGYVYFEEYAYSHQLSRADVTTVSTFIDLNITMLEDHEFVPLEVYTRHEIKDSGLL  697
            F FGGGYVYFEEYAYSHQLSRAD+TTVSTFIDLNITMLEDHEFVPLEVYTRHEIKDSGLL
Sbjct  525   FTFGGGYVYFEEYAYSHQLSRADITTVSTFIDLNITMLEDHEFVPLEVYTRHEIKDSGLL  584

Query  698   DYTEVQRRNQLHDLRFADIDTVI  720
            DYTEVQRRNQLHDLRFADIDTVI
Sbjct  585   DYTEVQRRNQLHDLRFADIDTVI  607
```

Figure S4 Comparison of the primary amino acid sequences of HSV-2, strain 333, amino acids 98–720 (Query) and simulated protein based on 4BOM template (Sbjct). Middle record is composed of amino acids, which are identical in Query and Subject.

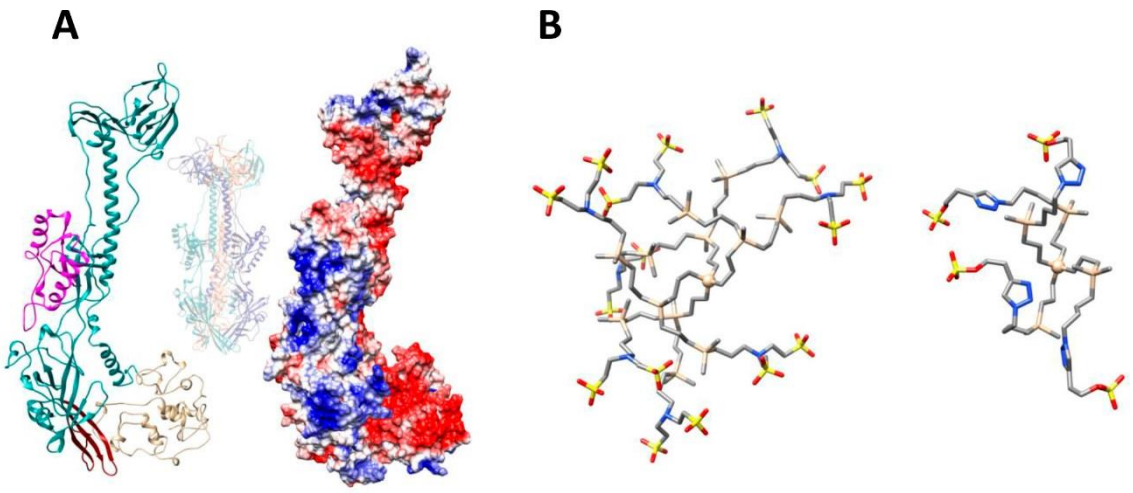

Figure S5 (A) Left: Equilibrated structure of the gB protein from HSV-2 (strain 333) (residues 98–904). Right: The same (including the view/orientation) just with visualized electrostatic potential on the molecular surface (blue color denotes high values of positively charged domains with potential +3 kT/e and higher and low values of electrostatic potential –3 kT/e and lower in rather anionic areas are in red). Middle – original gB trimer from HSV-1 (PDB: 4BOM) – full size figure is in supplementary information (Figure S2). (**B)** Representative conformations of the computer models of dendrimers G2-S16 (left), G1-S4 (right), simulated in salt water. Hydrogen atoms are omitted for the better clarity. The color coding is: C, grey; O, red; Si, beige; S, yellow; N, blue.

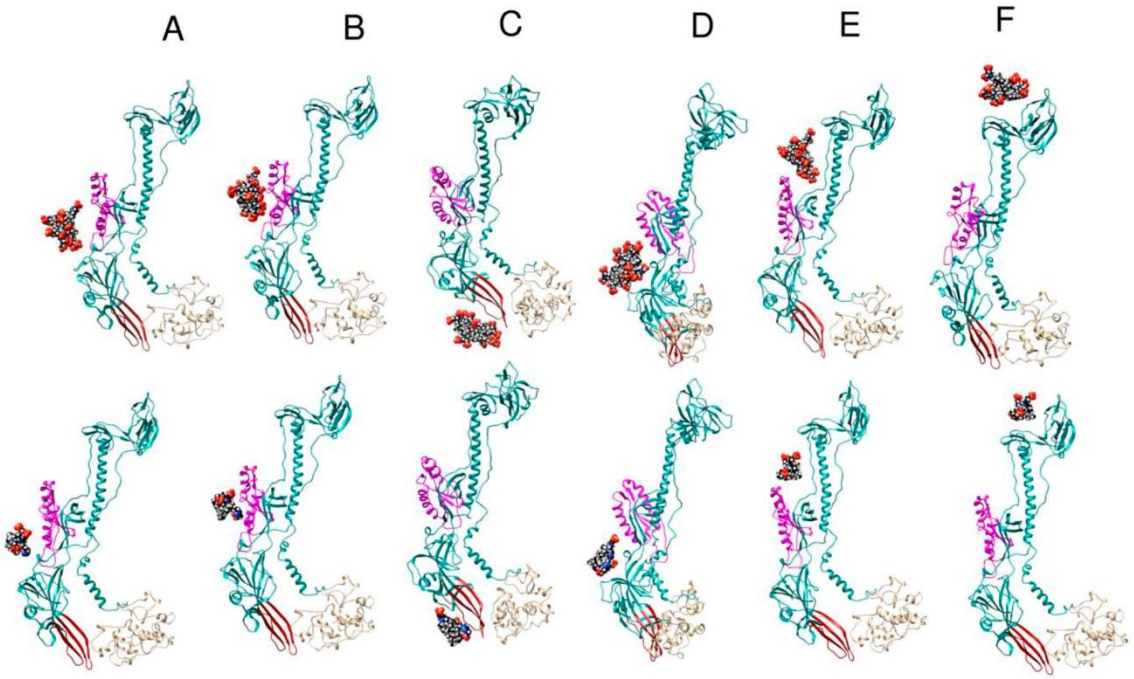

Figure S6 All the initial configurations of simulated G2-S16/gB (top), G1-S4/gB (bottom) systems.

Notes: The main part of the suggested binding interface for the gH–gL is highlighted in magenta. The putative fusion loops are in red and the C-terminal part comprising residues 721–904 is in tan. This part of the gB protein was not included in our gB template structure (4BOM), so we simulated it from the primary amino acid sequence just to "naturally" close this incomplete part. In reality, most of this gB part anchored in viral membrane has different tertiary structure. Atoms of dendrimer are colored as follows: C, black; O, red; Si, gray; S, yellow; N, blue; H, white.

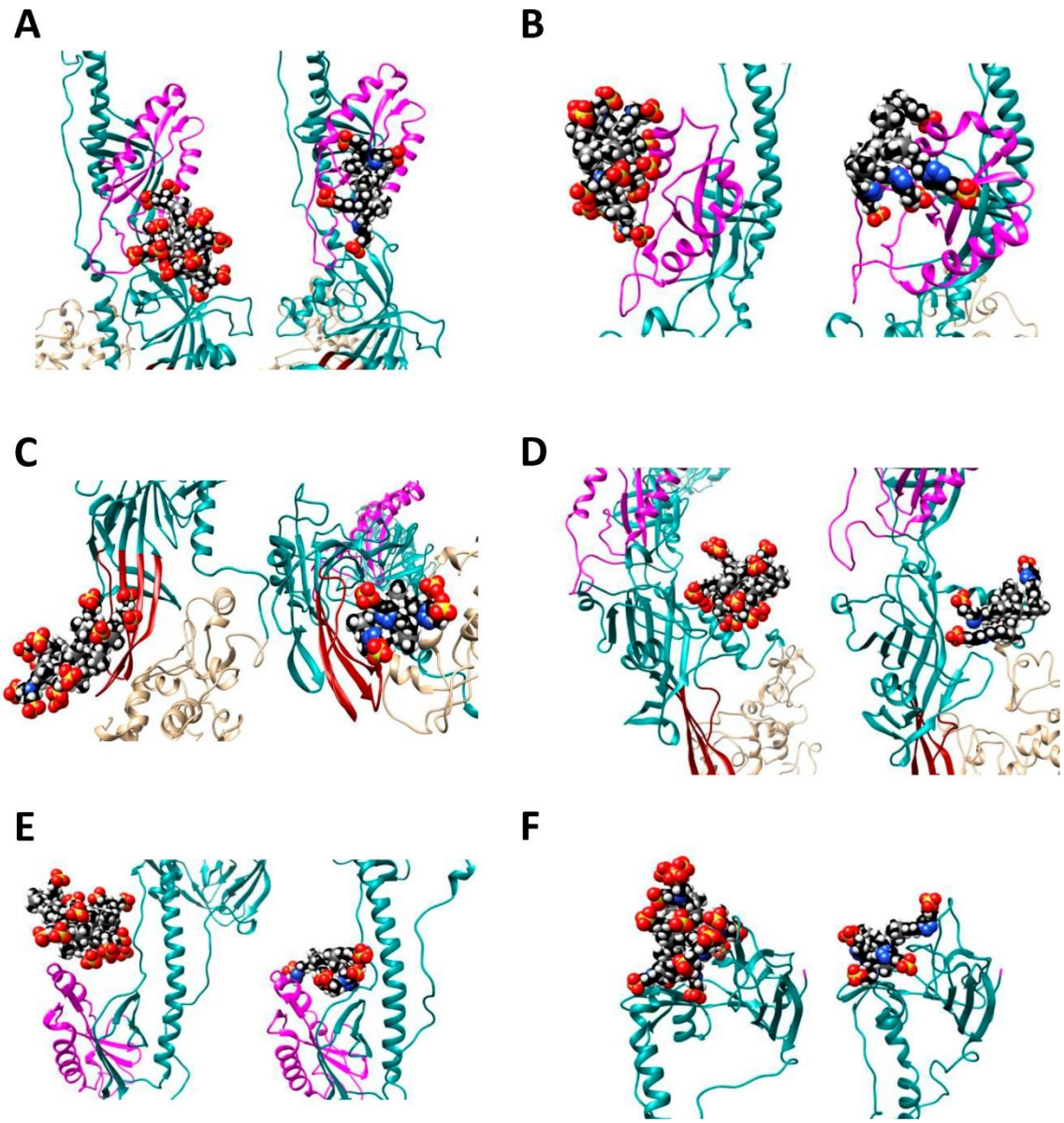

Figure S7 Detail view of the final G2-S16/gB (left), G1-S4/gB (right) systems.

Notes: (A) Case A (interaction at gH–gL binding area). **(B)** Case B (interaction at gH–gL binding area). **(C)** Case C (interaction with putative fusion loops). **(D)** Case D (cationic area above the fusion loops). **(E)** Case E (interaction at "pocket" near the top edge of the gH–gL binding site). **(F)** Case F (the top part of the gB protein or N-terminal area). Atoms of dendrimer are colored as follows: C, black; O, red; Si, gray, S, yellow, N, blue; H, white.

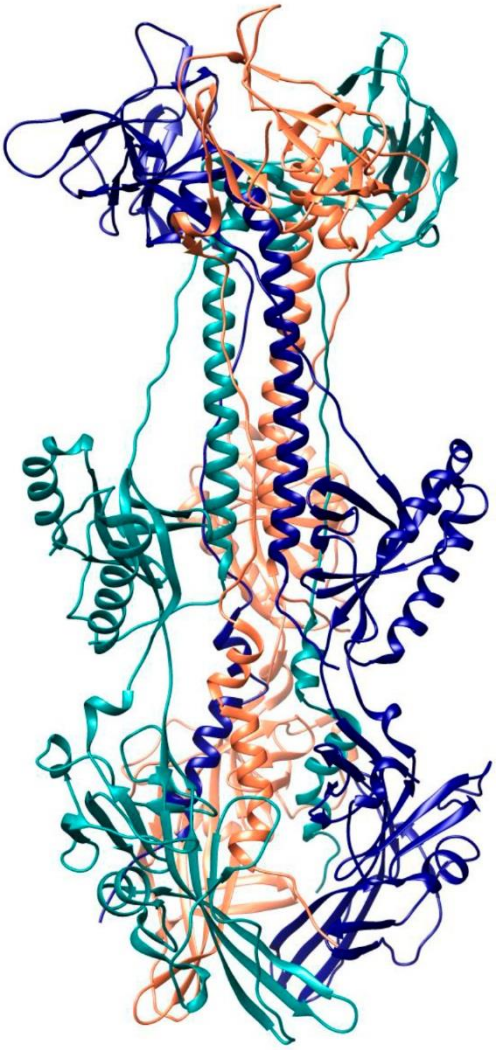

Figure S8 Visualization of the gB trimer from HSV-1 (PDB: 4BOM).

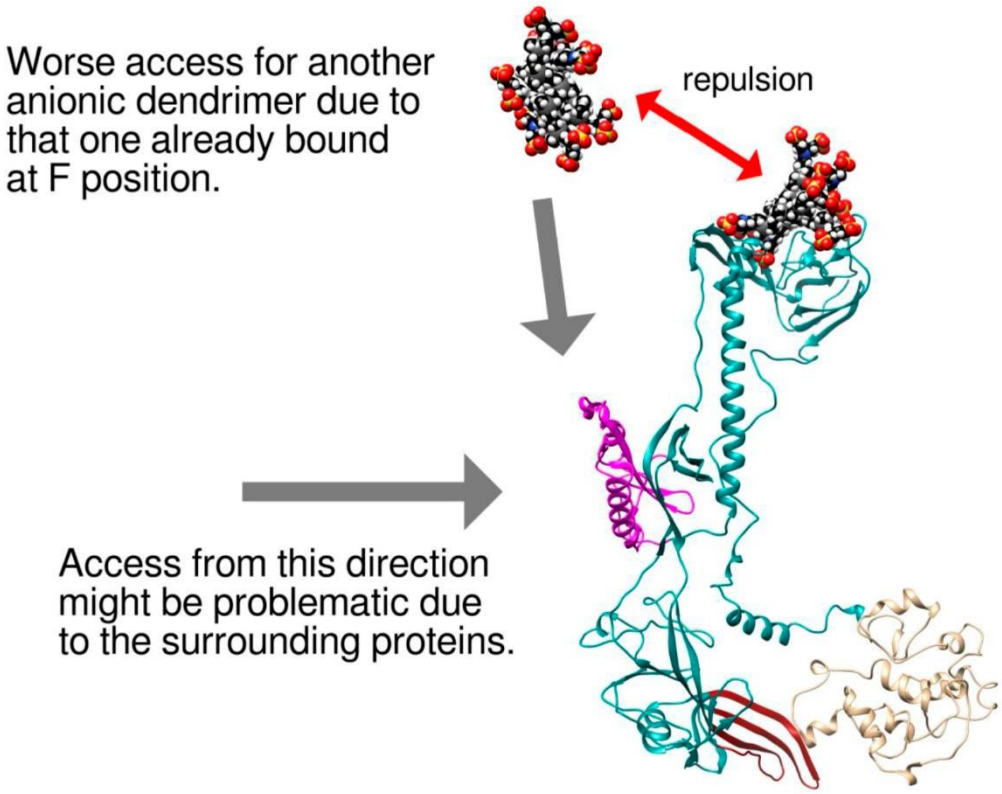

Figure S9 Illustration of disturbing role of already bound dendrimer at position F for access of the another dendrimer, which would like to reach gH–gL binding domain.

Note: In case of already visualized dendrimer G2-S16, this "autoblocking effect" will be stronger than in case of G1-S4 dendrimer.

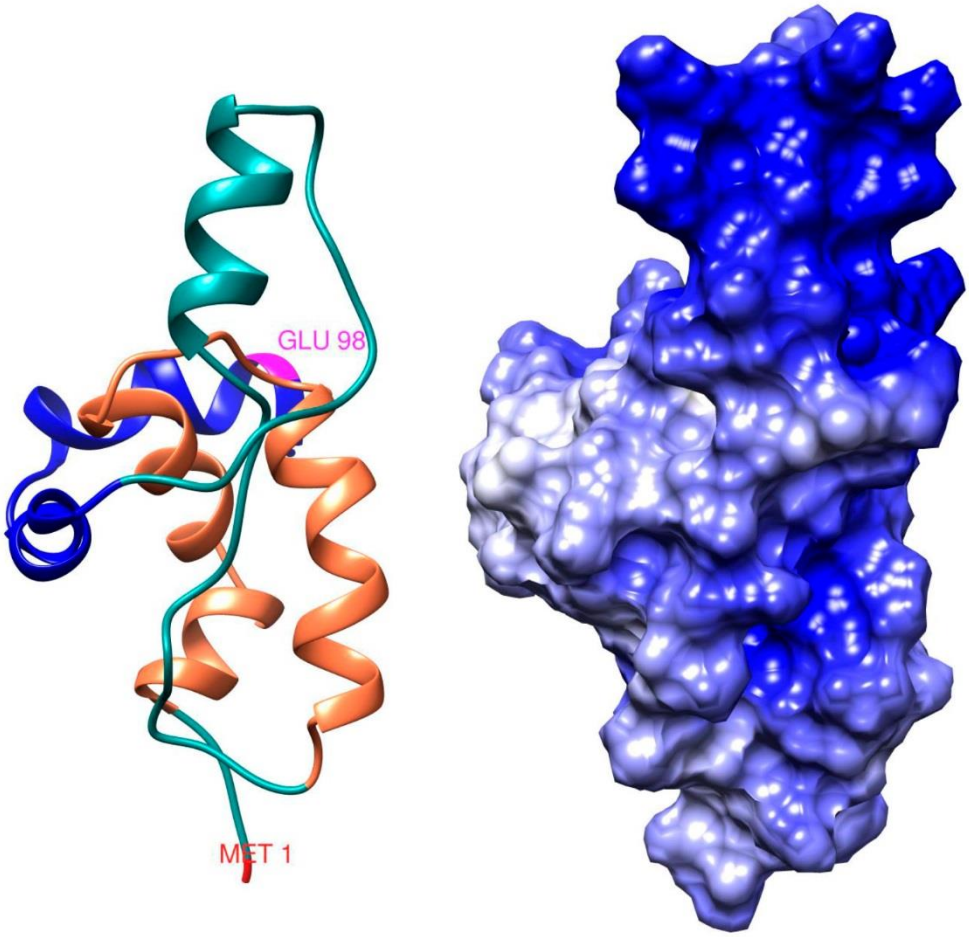

Figure S10 Approximate tertiary structure of N-terminal (amino acids 1–100) gB from HSV-2 (strain 333) obtained from the primary amino acid sequence using simulation (left), the same with electrostatic potential visualized on the surface (right) The white color denotes potential value 0 kT/e and the blue color means positive value +7 kT/e and higher. The effect of water was implicitly taken into account in this calculation.

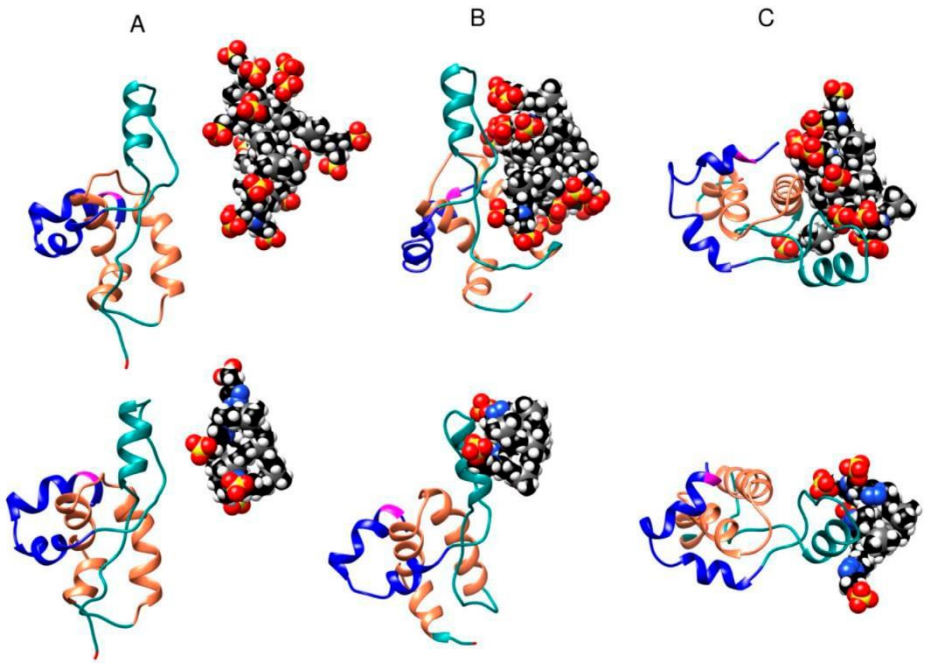

Figure S11 Simulated complexes N-terminal (residues 1–100) and dendrimers G2-S16 (top), G1-S4 (bottom).

Notes: **(A)** The initial state. **(B)** The final complex (side view). **(C)** The final complex (top view).

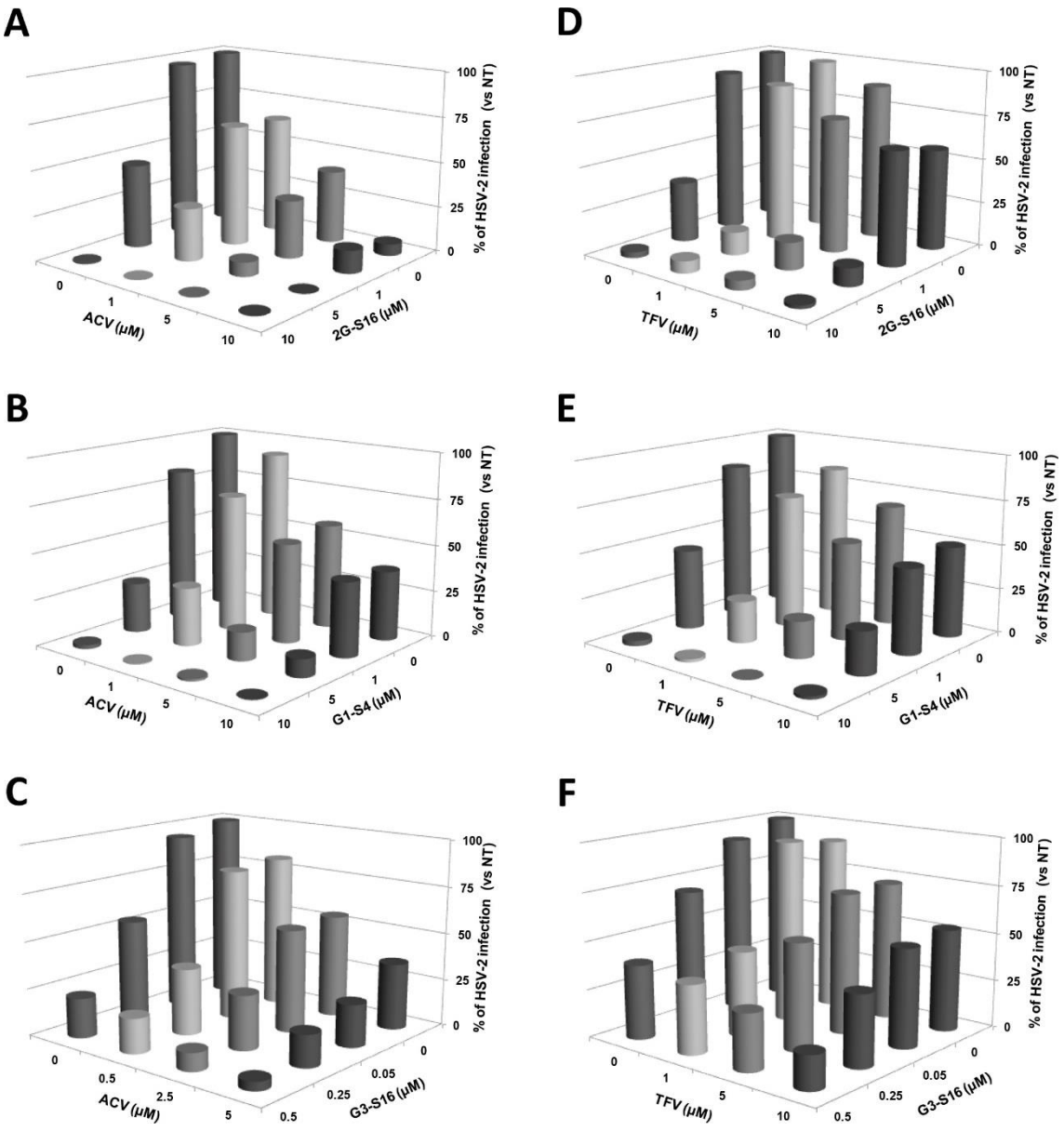

Figure S12 Activity profile of G2-S16 **(A–D),** G1-S4 **(B–E)**, and G3-S16 **(C–F)** alone or combined with ACV **(A–C)** or TFV **(C–E)** against HSV-2 strain 333 infection (% of infection was calculated as % of viral plaques vs nontreated cells) in Vero cell line. Vero cells were treated with different combinations of carbosilane dendrimers and ARV compounds 1 hour before HSV-2 infection. Each experiment was performed by triplicate. Data were represented as mean of three independent experiments.

Abbreviations: ACV, acyclovir; HSV-2, herpes simplex virus type 2; NT, nontreated; TFV, tenofovir.

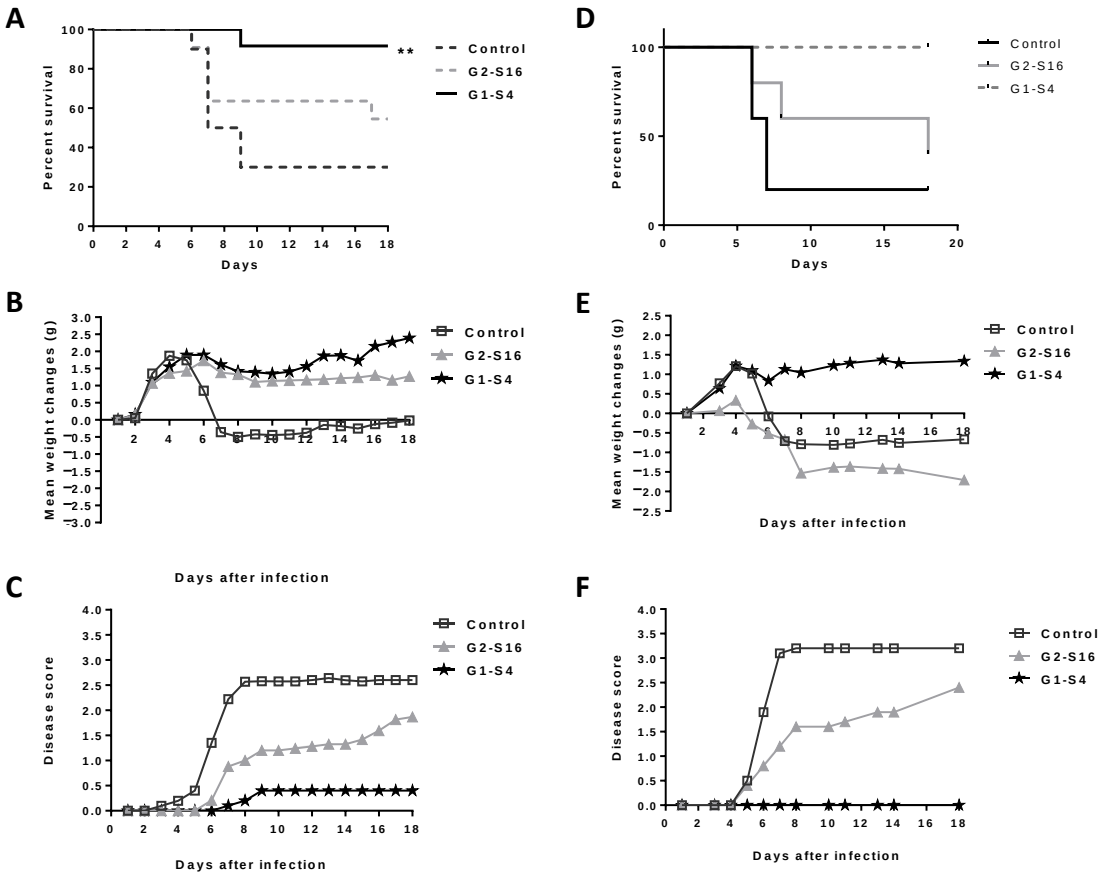

Figure S13 Polyanionic carbosilane dendrimers prevent rectal high-dose HSV-2 infection in BALB/c.

Notes: Male BALB/c mice **(A–C)** and female BALB/c mice **(D–F)** were rectally challenged with 10^5 PFU HSV-2 30 min after applying the indicated gel (five females and ten males per group). Mice were examined daily for body weight and genital pathology over 18 days. **(A and D)** The percentages of infection over time, based on symptoms, are shown for each treatment group. **(B and E)** Body weight changes were expressed as the mean values of ten animals in the same group. Each mean value was calculated by subtracting the weight at day 0 from the weight at day N after infection. **(C and F)** Clinical pathology was scored as described in the text for 16 days. Lesion scores were expressed as the mean values of five animals in the same group.

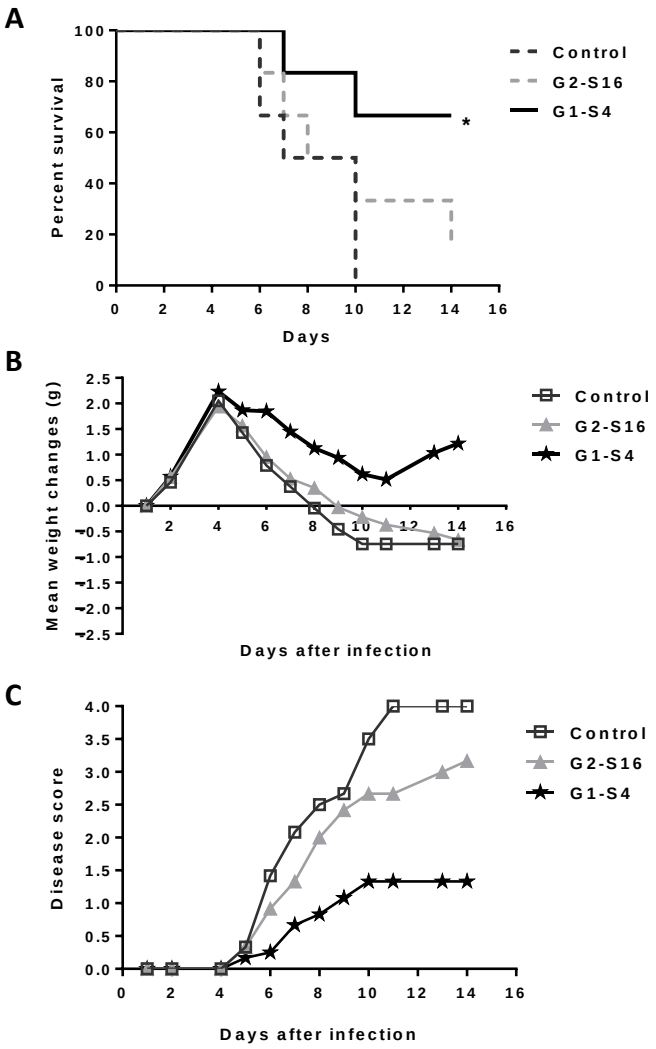

Figure S14 Polyanionic carbosilane dendrimers prevent rectal 1log high-dose HSV-2 infection in BALB/c.

Notes: BALB/c mice were rectally challenged with 10^6 PFU HSV-2 30 min after applying the indicated gel (five animals per group). Mice were examined daily for body weight and genital pathology over 18 days. **(A)** The percentages of infection over time, based on symptoms, are shown for each treatment group. G1-S4 was significantly protective (*P<0.05 vs control) **(B)** Body weight changes were expressed as the mean values of ten animals in the same group. Each mean value was calculated by subtracting the weight at day 0 from the weight at day N

after infection. **(C)** Clinical pathology was scored as described in the text for 18 days. Lesion scores were expressed as the mean values of five animals in the same group.